

NUMERICAL SIMULATION OF REACTING FLOWS FOR PROPULSION ENGINES

© V.N.Gavriliouk[†], V.Y.Gidasov[‡], I.E. Ivanov[‡], A.V.Khokhlov[†], U.G. Pirumov[‡], V.Y.Streltsov[†]

[†] – OOO “Nika Software”, Volokolamskoye sh. 4, Moscow, Russia

[‡] – Moscow Aviation Institute, Volokolamskoye sh. 4, Moscow, Russia

The present paper addresses to the questions of simulation of reactive flows in the elements of propulsion engines. Three tasks listed below are considered :

- Numerical modeling of experiments on ignition of reacting mixture in shock tube;
- Flame stabilisation behind a corner flame holder in a premixed benzene-air flow;
- Calculation of the mixing and combusting processes in a liner of air-breathing engine;

To solve the first task the 2D unsteady Euler system is used [18]. Solution of the other tasks bases on the unsteady Favre averaged 3D Navier-Stokes system with energy and species transport equations and the heat transfer equation for a solid body in combination with the models of thermodynamic properties, phase transition models, models of impulse, energy and mass exchange between liquid and gas phases [13, 14].

1. Introduction

The method of simulation of reacting flows of gas-spray mixtures proposed combines the methods of solution of RANS with k- ϵ turbulence model, methods for calculation of boundary layer, algorithms for calculation of droplets in spatial flow of reacting gas with heat and mass exchange, methods for calculation of equilibrium and kinetic reactions and universal approach to calculation of thermodynamic and diffusive properties.

Influence of turbulence on the combustion process is accounted in the frame of solution of averaged equations with turbulence model, which refers to Boussinesque approach. According the hypothesis of Spalding, the mixing process limits an amount of reacting substance, which can be derived accounting the averaged parameters of turbulent flow. The simplest implementation of such model is well-known eddy break-up approach for equilibrium reactions [1] and its modification for kinetically reacting fluid referred to as “eddy dissipation concept” [2]. The essence of the last is to set some relations between the averaged parameters of turbulence, such as k and ϵ , and rates of chemical reactions. The method present follows a modification of such approach since it yields fully conservative procedure.

2. The Mathematical Formulation of the Flow of Gas-Spray Mixture

2.1. The Model of Gas Phase

The method of calculation of steady/unsteady turbulent reacting gas with spray admixture is based on solution of Favre averaged Navier-Stokes equations, equations of k- ϵ turbulence model, transport

equation for total chemical-thermal enthalpy and several transport equations for mass fractions of reactants.

$$\frac{\partial p}{\partial t} + \frac{\partial \rho u_i}{\partial x_i} = S_m, \quad (1)$$

$$\frac{\partial \rho u_i}{\partial t} + \frac{\partial \rho u_i u_j}{\partial x_j} + \frac{\partial p}{\partial x_i} = \frac{\partial}{\partial x_j} (\tau_{ij} + \tau_{ij}^R) + S_i, \quad i = 1, 2, 3, \quad (2)$$

$$\begin{aligned} \frac{\partial \rho H}{\partial t} + \frac{\partial \rho u_i H}{\partial x_i} + \frac{\partial}{\partial x_i} \left[-u_j (\tau_{ij} + \tau_{ij}^R) - \left(\frac{\mu}{Pr} + \frac{\mu_t}{Pr_t} \right) \left(\frac{\partial H}{\partial x_i} - \frac{\partial u^2}{2 \partial x_i} \right) \right] = \\ = \frac{\partial p}{\partial t} - \tau_{ij}^R \frac{\partial u_i}{\partial x_j} + \rho \varepsilon + S_H, \quad H = h + \frac{u^2}{2} \end{aligned} \quad (3)$$

$$\frac{\partial \rho k}{\partial t} + \frac{\partial \rho k u_i}{\partial x_i} = \frac{\partial}{\partial x_i} \left(\left(\mu + \frac{\mu_t}{\sigma_k} \right) \frac{\partial k}{\partial x_i} \right) + \tau_{ij}^R \frac{\partial u_i}{\partial x_j} - \rho \varepsilon, \quad (4)$$

$$\frac{\partial \rho \varepsilon}{\partial t} + \frac{\partial \rho \varepsilon u_i}{\partial x_i} = \frac{\partial}{\partial x_i} \left(\left(\mu + \frac{\mu_t}{\sigma_\varepsilon} \right) \frac{\partial \varepsilon}{\partial x_i} \right) + f_1 C_{\varepsilon 1} \frac{\varepsilon}{k} \tau_{ij}^R \frac{\partial u_i}{\partial x_j} - f_2 C_{\varepsilon 2} \frac{\rho \varepsilon^2}{k}, \quad (5)$$

$$\frac{\partial \rho y_m}{\partial t} + \frac{\partial \rho y_m u_i}{\partial x_i} = \frac{\partial}{\partial x_i} \left(\frac{\mu}{Pr} + \frac{\mu_t}{Pr_t} \right) \frac{\partial y_m}{\partial x_i} + S_{y,m}, \quad m = 1, 2, \dots, N_c, \quad (6)$$

Here $\tau_{ij} = \mu s_{ij}$, $\tau_{ij}^R = \mu_t s_{ij} - \frac{2}{3} \rho k \delta_{ij}$, $s_{ij} = \frac{\partial u_i}{\partial x_j} + \frac{\partial u_j}{\partial x_i} - \frac{2}{3} \delta_{ij} \frac{\partial u_k}{\partial x_k}$, $S_m = \sum_m S_{m,m}$ - source due to the phase change, $S_i = \rho \mathbf{g}_i + S_{di}$ - influence of buoyancy force and source of impulse of phase interaction, $S_H = \rho \mathbf{g}_i u_i + Q + S_{dh}$ - work of gravity force, thermal sources and source of phase interaction, $S_{y,m} = S_{m,m} + W_m$ - source of components in phase change and chemical reactions, $C_\mu, C_{\varepsilon 1}, C_{\varepsilon 2}, \sigma_k, \sigma_\varepsilon$ - constants of turbulence model, f_μ, f_1, f_2 - functions of laminar-turbulent transition, \mathbf{g} - acceleration of body force, H - total enthalpy per unit of mass, k - kinetic energy of turbulence, p - pressure, Pr - Prandtl number, Pr_t - turbulent Prandtl number, t - time, u_i - components of velocity, x_i - Cartesian coordinates, ε - rate of dissipation of turbulent energy, μ - dynamic viscosity, μ_t - turbulent viscosity, ρ - density, $\boldsymbol{\tau}$ - stress tensor, $\boldsymbol{\tau}^R$ - Reynolds stress tensor, y_m - mass fraction of m -th component.

Let us notice some important specifics of equations (1)-(6) and solution methods hereto.

Firstly, the density of a gas does not follow from the solution of (1)-(6), but is calculated from the state equation of generalized form $\rho = F(P, H, y)$, how it follows from the certain implementation of thermodynamic system.

Secondly, the method was developed for turbulent flows. Accordingly, the simple and unambiguous hypothesis of $Le=1$ was adopted. Applying the Fick's law and this hypothesis it is possible to transform the energy conservation law to the form (3) that is consistent with wide range of turbulent flows.

Finally, the third important feature is the approximation of the source terms. To say nothing about the certain implementation, such approximation must satisfy the laws of conservation of substance, energy and impulse. Moreover, the precision of approximation of conservation laws in this case determines the general precision of the results and influences on the stability and convergence of the method.

The mesh used for discretization of the equations above is based on the technology of rectangular adaptive meshes, which provides the automatic mesh generation for objects with complex geometry [3]. Adaptation of the mesh to the surface accounts the direction of normal vector and variation of the cell volume of the cell adjacent to the surface. To construct the approximation the staggered finite-volume approach is used. This approach yields conservative schemes [3-7]. To resolve continuity and impulse equation the SIMPLE-like procedure is used. All spatial operators and convective terms are having the second order of approximation. Non-linear approximation of convective terms with limiter provides the monotonic properties of the scheme. To resolve the task of conjugated heat transfer the single system of discrete equation for fluid and solid is used.

The system of linear equations achieved after discretization and linearization of equations is solved using multigrid method [8]. Increasing the number of cells, this method provides close to linear growth of number of operations necessary. The procedure of construction of succession of meshes and corresponding systems of linear equations is fully automated, does not require discretization and makes a good use of the properties of rectangular adaptive mesh. For the sequence of meshes created the block procedure is implemented that provides the correspondence of variables with any cell in any mesh as well as the uniform procedure for the geometry of any complexity. The smoother is the relaxation method of Gauss-Seidel type that is stabilized upon necessity by local iterative parameter.

To solve the conjugated heat transfer problem, the heat transfer equation is used in combination with interface condition that provides equality of the heat flows at solid/fluid boundary.

Special feature of the method is the boundary layer solver, which is based on the integration of the boundary layer equations with boundary conditions at the wall and conventional external boundary. It provides the calculation of friction and heat transfer factors, and unlike the traditional wall functions the integration of the boundary layer is performed numerically in each point at the surface. Such approach relaxes the requirements to the density of mesh near the wall and provides interfacing at greater y^+ .

2.2. Calculation of Thermodynamic and Thermophysical Properties.

Thermodynamic properties of reacting gas are determined using the model of multi-component perfect gas in the frame of hypothesis of uniform population of energy levels in accordance with all internal degrees of freedom of molecules and atoms [9].

In this case the specific thermodynamic Gibbs's potential has the following form:

$$G(p, T, \gamma) = \sum_{i=1}^{N_c} \gamma_i [RT \ln(p\gamma_i / p_0 \sum_{j=1}^{N_c} \gamma_j) + G_i^0(T)], \quad (7)$$

Here: R - universal gas constant, γ_i - molar-mass concentration of i -th component, $p_0 = 101325 \text{ Pa}$ - standard pressure, $G_i^0(T)$ - standard molar Gibb's potentials of separate components, which are related to the standard reduced potentials $\Phi_i^0(T)$ according [9]:

$$G_i^0(T) = \Delta_f H_i^0(T_0) - [H_i^0(T_0) - H_i^0(0)] - T\Phi_i^0(T), \quad (8)$$

Here $T_0 = 298,15 \text{ K}$ - standard temperature, $H_i^0(0)$ - standard enthalpy $H_i^0(T)$ at absolute zero, $\Delta_f H_i^0(T_0)$ - enthalpy of production of i -th component standard temperature. Similarly, thermodynamic properties of liquid phase are described with molar Gibb's potential:

$$G_l(p, T) = G_l^0(T) + \mu_l(p - p_0)[\rho_l^0(T)]^{-1}, \quad (9)$$

Here $\rho_l^0(T)$ - density of liquid phase, μ_l - molecular weight of liquid component.

To calculate $\Phi_i^0(T)$ the polynomial proposed in [9] are used, which are the approximation of the reference data on the reduced standard potentials of various gases and condensates.

Other thermodynamic properties are derived from Gibbs's potentials and its partial derivatives by pressure and temperature (for instance, specific volume $v = \left[\frac{\partial G}{\partial p} \right]_T = \frac{RT}{p} \sum_{(i)} \gamma_i$, enthalpy

$$h = G - T \left(\frac{\partial G}{\partial T} \right)_p, \text{ heat capacity } C_P = -T \left(\frac{\partial^2 G}{\partial T^2} \right)_p.$$

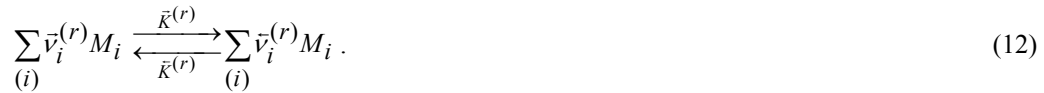
Viscosity is calculated using the formula of Wilkey, and heat conductivity using the formula of Maason and Saxen with correlation of Eiken [10]:

$$\eta = \sum_{(i)} \eta_i (\gamma_i / B_i) \quad , \quad B_i = \sum_{(j)} A_{ij} \gamma_j, \quad A_{ij} = [1 + (\eta_i / \eta_j)^{1/2} (\mu_j / \mu_i)^{1/4}]^2 [8(1 + \mu_i / \mu_j)]^{-1/2} \quad (10)$$

$$\eta_i = \frac{5}{16} \left[\frac{\mu_i RT}{\pi} \right]^{1/2} \left[N_A \sigma_i^2 \Omega_i^{(2,2)*} \right]^{-1}, \quad \lambda = \sum_{(i)} \eta_i (1,32c_{pi} + 0,45R / \mu_i) (\gamma_i / B_i). \quad (11)$$

Parameters of interaction potentials of the same molecules $\sigma_i, \varepsilon_i, \delta_i$ and approximation of Brockau for the calculation of collision integrals of Schtockmyer $\Omega_i^{(2,2)*}$ are from [10].

Kinetic reactions in gas phase are described with the multi-stage reversible mechanism:



Here: r – number of the reaction, $\bar{v}_i^{(r)}$ - stoichiometric coefficients, M_i - symbols of chemical substances. Relations for W_i , according the mechanism (12), are the following [11]:

$$W_i = \sum_{(r)} (\bar{v}_i^{(r)} - \bar{v}_i^{(r)}) (\bar{W}^{(r)} - \bar{W}^{(r)}), \quad \bar{W}^{(r)} = \bar{K}^{(r)}(T) \exp \left[\sum_{(i)} \bar{v}_i^{(r)} \ln(\rho \gamma_i) \right]. \quad (13)$$

For described mechanism (12)-(13) to match the thermodynamics described with Gibbs's potentials (7), the following relation between reaction rates and each pair of mutually reverse reactions (12) is required:

$$\frac{\bar{K}^{(r)}(T)}{\bar{K}^{(r)}(T)} = \exp \left[\sum_{(i)} (\bar{v}_i^{(r)} - \bar{v}_i^{(r)}) \left(\frac{G_i^0(T)}{RT} + \frac{\ln RT}{p_0} \right) \right]. \quad (14)$$

To approximate the dependency of reaction rates of forward reactions from temperature the generalised Arrhenius relation [11] is used:

$$K(T) = A \exp \left(-\frac{E}{RT} + n \ln T \right) \quad (15)$$

2.3. The Model of Aerodynamic Resistance and Heat-mass exchange of droplets

Parameters of separate droplet in the flow of a gas are described with the following system:

$$\frac{dx_{li}}{dt} = u_{li}; \quad \frac{du_{li}}{dt} = \dot{u}_{li} = \frac{u_{li} - u_i}{\tau_v}; \quad \frac{dm_l}{dt} = \dot{m}_l; \quad \frac{de_l}{dt} = \dot{e}_l. \quad (16)$$

Here m_l , e_l - mass and internal energy of the droplet, x_{li} , u_{li} - position and velocity of the droplet in i -th direction. To calculate τ_v , \dot{m}_l , \dot{e}_l the semi-empiric model of quasi-stationary evaporation of separate droplet in the multi-component gas in continuum regime is used [12]. This model was tested in the works [13,14].

2.4. Kinetic model of kerosene combustion

To simulate the process of combustion of evaporated kerosene the effective reaction $C_{10}H_{22} + 15.5 O_2 \xrightarrow{\leftarrow} 10 CO_2 + 11 H_2O'$ was used. The rate of the reaction was determined using the data from [11]. Combustion products CO_2 and H_2O' are the pseudo-substances with the same composition matrix that of water and carbon dioxide, but with different thermodynamic properties. Thermodynamic properties of combustion products were chosen so that the heat production calculated

in effective reaction matches the heat production determined by detailed mechanism of combustion for lean mixtures.

2.5. Interaction of the models

One of the important questions is the agreement of the combination of the separate models described above. Accordingly, the satisfaction of conservation laws was selected as the criterion of correctness of the interfaces. To organise such interface the special numerical technique was used.

For instance, the source terms of the equations (1)...(6) are written in the following form:

$$S_{m,m} = -\sum_l n_l \dot{m}_l y_{ml}, \quad S_{di} = -\sum_l (n_l \dot{m}_l u_{l,i} + n_l m_l \dot{u}_{li}), \quad S_{dh} = -\sum_l n_l [\dot{m}_l (e_l + \frac{v_l^2}{2}) + m_l (\dot{e}_l + v_{li} \dot{v}_{li})], \quad (17)$$

here n_l - per-count density of l -th class of droplets, y_{ml} - mass fraction of m -th component in evaporation products of droplets.

Additionally, the possibilities of precise integration of the finite-volume approach were used.

Equilibrium model does not require additional efforts to provide conservation, because all products are the result of the local ratio of the reactants. Alternatively, for the kinetic model the approach related to the physical splitting is implemented (see [15]):

$$\frac{\partial \rho y_m}{\partial t} + \frac{\partial \rho y_m u_i}{\partial x_i} = \frac{\partial}{\partial x_i} \left(\frac{\mu}{Pr} + \frac{\mu_t}{Pr_t} \right) \frac{\partial y_m}{\partial x_i} + S_{y,m} + \rho \frac{\hat{y}_m - y_m}{\Delta t}, \quad (18)$$

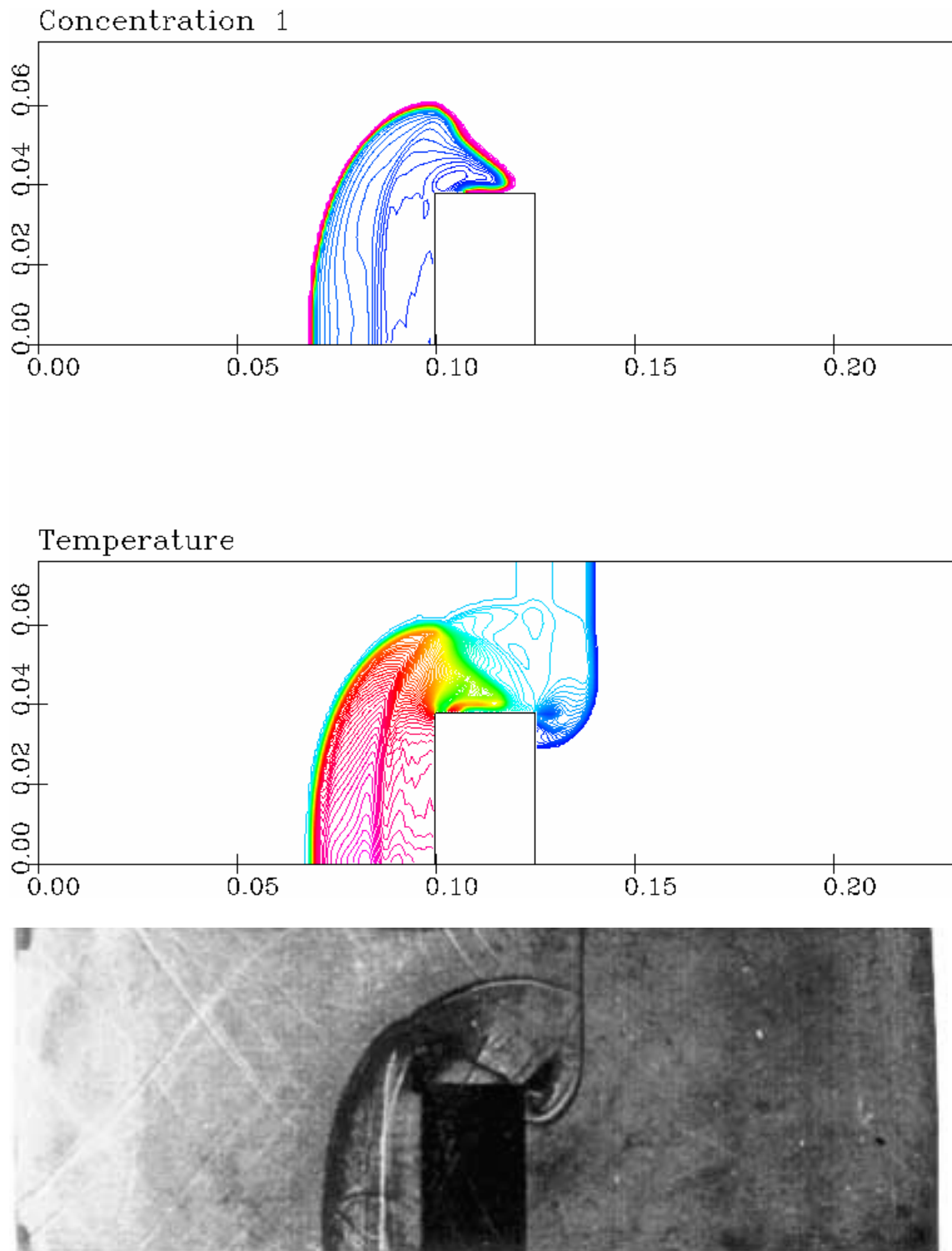
$$\frac{\partial \rho \hat{y}_m}{\partial t} = W_m, \quad m = 1, 2, \dots, N_c. \quad (19)$$

Here, for one step of transport equations (18), the several time steps for chemical kinetics (19) can be performed, relaxing the time stepping limitation.

3. The Examples of Calculations

3.1. Numerical modeling of experiments on ignition of a reacting mixture in the shock tube

Numerical modeling physical experiments in shock tubes on research of diffraction of a shock wave on a rectangular obstacle in reacting gas environment has been made. The shock tube has a cross-section of 38 x 76 mm. The obstacle represents a rectangular block in height equal to a half of the height of the channel and in width equal to the width of the channel. For modeling the chemical transformations of gaseous component the detailed kinetic mechanism describing burning of a hydrogen-oxygen-argon mixture, consisting of 19 reversible reactions and including 10 component was used. The initial pressure was 5.3 KPa, the Mach number on a falling shock wave 2.5. The distribution of the gaseous water and temperature can be seen in Fig. 1. Settlement with great dispatch wave structure of current which consists of a passing shock wave, a reflected shock wave, a front of burning and a front of a detonation wave, which coincides with high accuracy with observable in experiments is obtained.



Thomas, Ward, Williams, Barbey // Shock Waves 2002

Fig. 1. Comparisons of schlieren images and numerical results

3.2 The Stabilisation of Premixed Flame with the Corner Flameholder

The example below shows the flame stabilisation behind the corner flameholder located in the premixed benzene-air flow. It refers to the experimental measurements of the work [16]. Authors

measured the parameters of turbulence and temperature profiles. These data was selected for the validation of the model in the case of premixed combustion.

Experimental rig was the rectangular channel with the corner flameholder inside. Since the channel was rather narrow, and it was impossible to neglect the influence of the side walls, and the calculation was 3D. It is also important to mention that the ends of the flameholder were at some distance from the side wall, and this was necessary to account in calculation to achieve correct result.

The simplified kinetic mechanism of one conventional reaction was used in the calculation. Setting the initial and boundary conditions the data on the measured parameters of turbulence was used. Inlet flow of benzene-air mixture had the temperature of 412 K, velocity of 150 m/s at atmospheric pressure and air excess factor of $\alpha = 1.5$

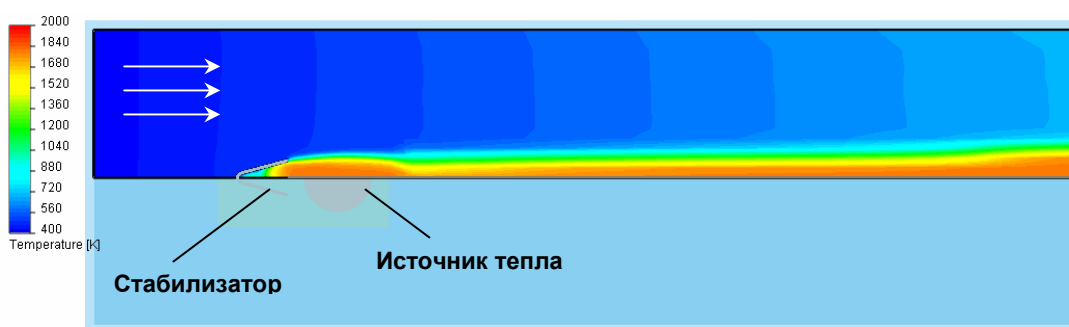


Fig 2 scheme of the calculation combined with the temperature distribution in the symmetry plane of the channel.

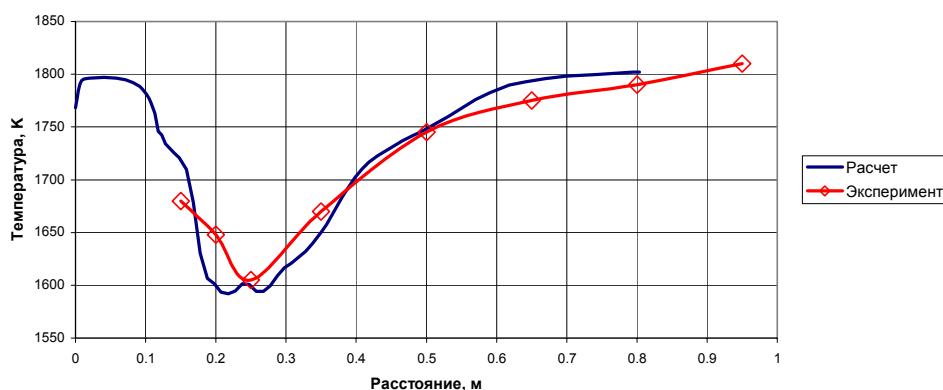


Fig 3 Temperature profile plotted along the central line of the rectangular channel.

Scheme of the calculation can be seen in Fig. 2. The calculation was performed using an unsteady method with accumulation of average temperature in time. Initial approach was the steady flow of cold mixture and after “ignition” the calculation was prolonged until stabilization of average temperature field. “Ignition” of mixture was performed enabling temporary the heat source located in the reverse flow zone.

Comparing the calculated and experimental temperature profiles shown in Fig. 3 one can see the good agreement of the calculated and measured size of the reverse flow zone, position of the maximal and minimal temperature, and it is possible to say that generally the simulation is correct.

3.3. Calculation of the Combustion Chamber of the Air-breathing Engine

Calculation of the combustion chamber of the engine was conducted to determine the heat loads acting on the chamber's walls and estimate the emission of pollutants. After the series of calculation the recommendations on the optimisation of the geometry and working process necessary to reduce the emission of the pollutants were worked out.

Geometry of the model repeated even the small features of the design (Fig. 4). Setting the boundary conditions the specifics of air and fuel supply were accounted. Parameters of the flow in swirling head of the frontal system were calculated in the same run. Generally, for the chamber the air and fuel flow were set. Spectra of the particles formed in the decay of the liquid film and the other initial parameters of the spray were taken from the experimental data. The field of each fraction of the spray was calculated on the independent Lagrange mesh formed by the particle trajectories in each fraction. Such number of trajectories was selected so that they uniformly and with appropriate density were filling the volume of presence of each fraction.

In particular, the example below shows the calculation for the inlet temperature of 744 K, inlet pressure of 20 Bar, air flow of 1.2 kg/s and fuel consumption of 0.025 kg/s. The size of droplets was set in the range from 1.2 to 100 micron for 20 fractions. Each fraction was started from 30 points located at the conventional place of decay of the liquid film formed by the centrifugal sprayer with swirled internal flow. Start velocity of the reference trajectories was varied both by magnitude and inclination relative to sprayer's axis. The interaction between fractions was neglected as well as the influence of the radiation on the temperature of the droplets. Numerical mesh (Fig. 2.2) had 209542 cells. Time necessary for this run comprised 62 hours on the computer with Athlon XP 1900+.

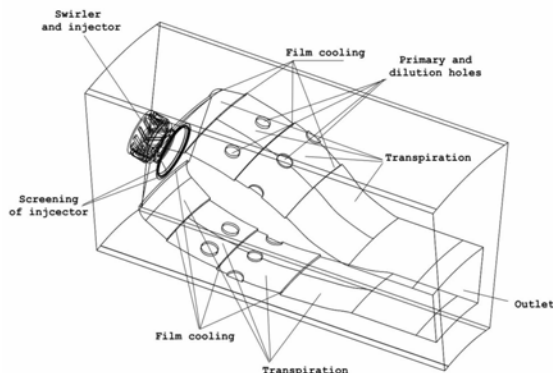


Fig. 4 Scheme of the chamber's sector

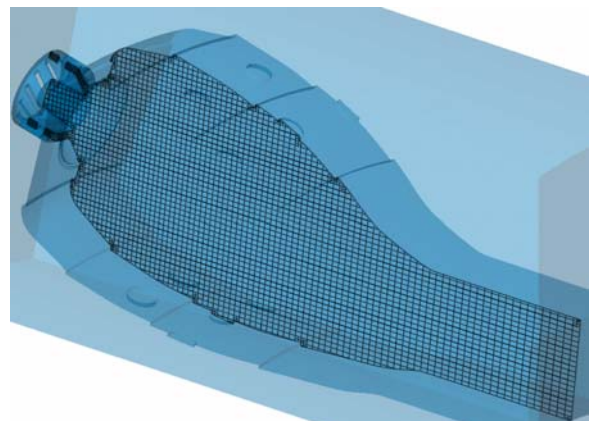


Fig. 5 Trace of the mesh in axial section

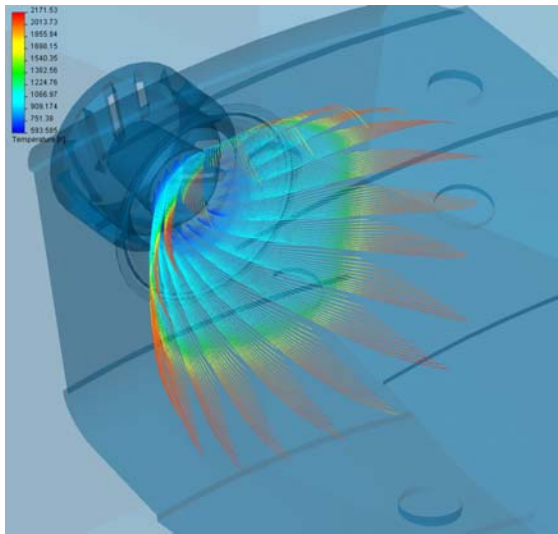


Fig. 6 Trace of one set of the reference trajectories used in the calculation

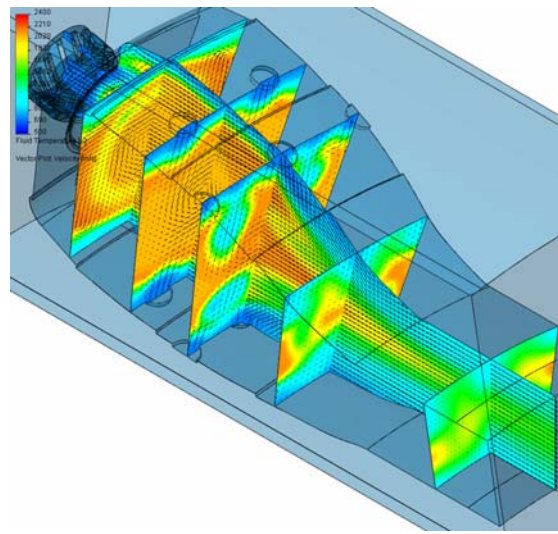


Fig. 7 Temperature distribution in set of the sections

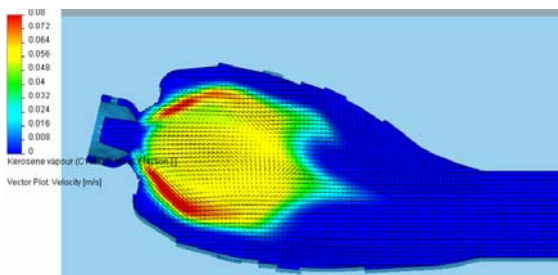


Fig. 8 Distribution of the gaseous kerosene in central section

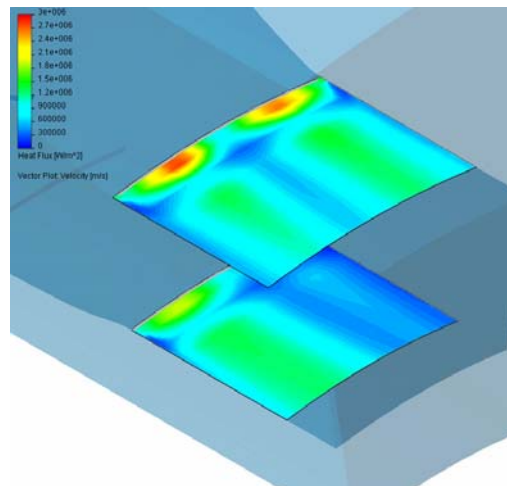


Fig. 9 Distribution of the heat flows at the exit walls

Series of figures 6-9 shows the results achieved. Fig. 6 shows the set of reference trajectories of evaporation kerosene droplets for 20 fractions emitted with one of the velocities. The end of the trajectory corresponds to the total evaporation of the droplet. Accordingly, the distribution of the gaseous kerosene can be seen in Fig. 8. Temperature distribution in the segment of annular chamber can be seen in Fig. 7, where the penetration of diluting clean air jets can be observed. Fig. 9 shows the calculated heat loads on the walls of the chamber. Where the temperature is high the peaks can be observed in the place of local stagnation of the flow near the fracture of the contour.

Estimation of the emitted pollutants at the exit of the chamber provides the basis for optimisation of the fuel and air supply from the point of view of the reduction of harmful emissions, nevertheless, preserving the high combustion completeness. Results of such calculations are in good agreement with

the emission characteristics of the similar devices [17]. In particular, calculated index of emission of nitrogen oxides is in the range from 14 to 30 g/kg_{fuel}

Conclusion

The method of calculation of the reacting gas-spray mixture is in satisfactory agreement with the experimental data and can be used in the development of different purpose combustion chambers. The method provides for the local, integral and emission characteristics of combustion chambers. If it would become necessary, it is possible to add the models of decay/coagulation, influence of radiative heat flows, apply more complex reaction mechanisms, etc. to achieve better results.

Acknowledgements

The research described was partially supported by the Russian Fund of Fundamental Research (grants N 03-01-00866-a and 04-01-81012-Бел2004_a).

References

1. Spalding D.B. Combustion and Mass Transfer. Pergamon Press, 1979.
2. Spalding D.B. Mixing and chemical reaction in steady confined turbulent flames //13th Symp. Comb., The Combustion Institute, Pittsburg, 1970. p. 649.
3. Gavrioliok V.N., Denisov O.P., Nakonechny V.P., Odintsov E.V., Sergienko A.A., Sobachkin A.A., Numerical Simulation of Working Processes in Rocket Engine Combustion Chamber. //IAF-93-S.463, October, 1993, Graz, Austria
4. Krulle, G., Gavrioliok, V., Schley, C.-A. and Sobachkin, A., Numerical simulation technology of aerodynamic processes and its applications in rocket engine problems // 45th Congress of the Int. Astronautical Federation, Jerusalem, Israel, October 9-14, 1994, IAF-94-S2.414, pp 1-12.
5. Hagemann, G., Schley, C.-A., Odintsov, E and Sobatchkine, A., Nozzle flow field analysis with particular regard to 3D-plug-cluster configurations. // 32nd AIAA/ASME/SAE/ASEE Joint Propulsion Conf., Lake Buena Vista, FL, July 1-3, 1996, AIAA-96-2954, pp 1-16.
6. Schley, C.-A., Deplanque, J., Merkle, C., Duthoit, V. and Gavrioliok, V., Fundamental and technological aspects of combustion chamber modelling. // Proc. 3rd Int. Symp. Space Propulsion, Beijing, China, August 11-13, 1997, pp 1-15.
7. Pavlov A.N., Sazhin, S.S., Fedorenko, R.P. and Heikal, M.R., A conservative finite difference method and its application for analysis of a transient flow around a square prism // Int. J. Numer. Methods Heat Fluid Flow, Vol. 10, No. 1, pp 6-46, 2000.
8. Trottenberg, U., Oosterlee, C.W., Schuller, A. with Brandt, A., Oswald, P. and Stuben. K., Multigrid, Academic Press, San Diego, 2001.
9. Gurvich L.V. et al. Thermodynamical properties of selected substances. Handbook in 4 V., M. Nauka, 1982.
10. Reid R., Prausnitz J., Sherwood T. The Properties of gases and liquids. New York: McGraw-Hill Book Company, 1977.
11. Physical-chemical processes in gas dynamics. Handbook V. 2: Physical-chemical kinetics and thermodynamics //Editors Cherny G.G., Losev S.A. – M.: Scientific-Editorial Center of Mechanics. 2002. 368 p.
12. Faeth G.M. Evaporation and combustion of sprays //Prog. Energy Combust. Sci. 1983. v.9. N 1/2. P. 1-76.
13. Volkov V.A., Musin V.R., Pirumov U.G., Prokhorov M.B. and Strel'tsov V.Yu. Numerical modelling of carbon monoxide neutralization by metered water injection into a high-temperature mixture of combustion products //Izv.Rossiiskoi Akad. Nauk,Mekh. Zhidk. Gaza.1993.N 6.P. 96-106.
14. Volkov V.A., Gidasov V.Yu., Pirumov U.G., Strel'tsov V.Yu. Numerical Simulation o Flows of Reacting Gas-Droplet and Gas Mixtures in Methanol Ignition Experiments// High Temperature, Vol. 36. № 3. 1998, pp. 401-411.
15. Shang H.M. et. al. Investigation of Chemical Kinetics Integration Algorithms for Reacting Flows. //AIAA Paper 95-0806, 1995.
16. Solntsev V.P., Golubev V.A. Research of process of combustion of a benzene-air mixture in conditions of interaction of the turbulent track formed by stabilizers / News of higher educational institutions MHE the USSR, a series " Aviation technics ", 1959
17. Lister D. ICAO Engine Exhaust Emission Data Bank, update 2003, based on ICAO doc 9646, 1995.
18. Gidasov V.Yu., Ivanov I.A., Kryukov I.A. Numerical modelling of initiation of a detonation in the focusing channel // Mathematical modeling. V. 4. N 12, 1992. P. 85-88.